

Amplification of frequency upshifted radiation by cold relativistic guided electron beams

A. Fruchtman

Center for Plasma Physics, Racah Institute of Physics, Hebrew University of Jerusalem, Jerusalem, Israel

L. Friedland

Center for Plasma Physics, Racah Institute of Physics, Hebrew University of Jerusalem, Jerusalem, Israel
and Applied Physics, Yale University, New Haven, Connecticut 06520

(Received 21 December 1981; accepted for publication 3 February 1982)

An amplifier on cold, relativistic, guided electron beams is considered. The problem is reduced to a set of first-order, linear, ordinary differential equations. The dispersion relation governing the stability of the system is derived and its solutions are studied numerically. The results of the calculations show that in the submillimeter regime, the spatial growth rates in the system may be comparable to those predicted for Raman-free electron lasers.

PACS numbers: 42.55.Bi, 41.70. + t, 41.80.Dd

I. INTRODUCTION

A great experimental and theoretical effort has been made in recent years in developing powerful sources of coherent radiation, using relativistic electron beams. In free electron lasers, for example, the beams are scattered on periodic magnetostatic structures and amplify electromagnetic signals at a wavelength $\lambda \simeq \lambda_0/2\gamma^2$, where λ_0 is the spatial period of the scattering magnetic field and $\gamma = [1 - (v/c)^2]^{-1/2}$ is the relativistic factor, v being the velocity of the beam.¹ These devices have shown a capability for operation in a wide frequency range from millimeter waves to infrared. This broad spectrum of operation is obtained by changing the energy of the electron beam, thus varying the amount of the Doppler upshift in frequency, which is proportional to γ^2 .

A different mechanism of amplification of a high-frequency radiation was suggested by Hirshfield *et al.*,² who demonstrated the possibility of exploiting the cyclotron maser type instability at Doppler upshifted frequencies. In contrast to free electron lasers, the mechanism discussed² does not need to have magnetostatic scattering and relies on the electron beam gyrating in a strong uniform magnetic field. The amplification of an electromagnetic signal is expected at frequencies $\omega \simeq 2\gamma^2\Omega$, where $\Omega = eB/mc\gamma$ is the relativistic electron cyclotron frequency. As is common to many studies of cyclotron masers, the electron beam² was assumed to have the following velocity distribution function

$$f(v_x, v_y, v_z) = f(|\mathbf{v}_\perp|, v_z), \quad (1)$$

where \mathbf{v}_\perp is the velocity perpendicular to the magnetic field. Thus the direction of \mathbf{v}_\perp was assumed to be distributed uniformly. In this case the transverse and longitudinal electromagnetic modes in the system are decoupled and, as was shown,² one of the transverse modes is spatially unstable.

In the present paper we are also exploiting the idea of using relativistic electron beams in strong uniform magnetic fields. In contrast to Ref. 2, however, we consider a different velocity distribution function. We assume that initially, at the entrance into the interaction region, the distribution function is

$$f(v_x, v_y, v_z)|_{z=0} = A\delta(v_x - v_{x0})\delta(v_y - v_{y0}) \times \delta(v_z - v_{z0}), \quad (2)$$

where δ is the Dirac function. The interaction of such a beam with radiation in a uniform axial magnetic field can be described by the cold fluid model, as opposed to case (1), where the study of the interaction of the beam with radiation requires the Vlasov description.² In Sec. II we will derive a simple set of equations describing the evolution of the electromagnetic field along the device, by using a method similar to that applied recently to free electron lasers.³ In Sec. III, we will consider the momentum equation for the beam, which will determine the current sources in the field equations. In Sec. IV, we will reduce the dispersion relation governing our system and demonstrate that the cold beam (2) couples the longitudinal and transverse modes. This effect results in an enhanced spatial growth in the amplifier, as will be demonstrated in Sec. IV, where we will present numerical examples and compare our results with the results of Hirshfield *et al.*² and those predicted for free electron lasers, operating in a comparable regime.

II. FIELD EQUATIONS

Consider an electromagnetic wave propagating along a relativistic cold electron beam, gyrating in a uniform magnetic field $\mathbf{B} = B_0\hat{\mathbf{e}}_z$. Adopting a one-dimensional model, we can describe the electromagnetic fields $\mathbf{E}(z, t)$ and $\mathbf{B}(z, t)$ by the system of Maxwell equations:

$$ce_z \times \frac{\partial \mathbf{B}_\perp}{\partial z} = \frac{\partial \mathbf{E}_\perp}{\partial t} - 4\pi eN \mathbf{V}_\perp, \quad (3)$$

$$-ce_z \times \frac{\partial \mathbf{E}_\perp}{\partial z} = \frac{\partial \mathbf{B}_\perp}{\partial t}, \quad (4)$$

$$\frac{\partial E_z}{\partial z} = -4\pi eN, \quad (5)$$

$$B_z = 0. \quad (6)$$

Here $\mathbf{V}(z, t)$ is the velocity of the electrons and N is the electron density, satisfying the continuity equation

$$\frac{\partial N}{\partial t} + \frac{\partial}{\partial z} (NV_z) = 0. \quad (7)$$

The subscript \perp in Eqs. (3) and (4) describes components of the electromagnetic field transverse to the z axis.

We are considering a stationary amplifier problem, namely, introduce an electromagnetic perturbation of frequency ω at $z = 0$ and solve for the electromagnetic field in the device as a function of z . Consistent with this problem we write

$$\mathbf{E}(z,t) = \text{Re} \left(\frac{mc^2}{e} \mathbf{a}(z) e^{i\omega(z/c - t)} \right), \quad (8)$$

$$\mathbf{B}(z,t) = \text{Re} \left(\frac{mc^2}{e} \mathbf{b}(z) e^{i\omega(z/c - t)} \right), \quad (9)$$

$$\mathbf{V}(z,t) = \mathbf{V}_0(z) + \text{Re}(\mathbf{v}(z) e^{i\omega(z/c - t)}), \quad (10)$$

$$N(z,t) = N_0 + \text{Re}(n(z) e^{i\omega(z/c - t)}), \quad (11)$$

where $N_0 = \text{const}$ and $\mathbf{V}_0(z)$ are the density and the velocity field characterizing the beam when the electromagnetic wave is absent. Note that in Eqs. (8) and (9) we are considering only rightward propagating waves, which is consistent with the amplifier problem considered in this paper. Equations (3) and (4) can be now combined and yield on linearization

$$\frac{d^2 \mathbf{a}_\perp}{dz^2} + 2i \frac{\omega}{c} \frac{d\mathbf{a}_\perp}{dz} = i \frac{\omega}{c^4} (\omega_p^2 \mathbf{v}_\perp + \mathbf{V}_{0\perp} n), \quad (12)$$

where $\omega_p^2 = 4\pi e^2 N_0/m$. Similarly Eq. (5) reduces to

$$\left(i \frac{\omega}{c} + \frac{d}{dz} \right) a_z = -\frac{n}{c^2}, \quad (13)$$

and the linearized continuity Eq. (7) becomes

$$\frac{1}{c} \left[i\omega \left(\frac{V_{0z}}{c} - 1 \right) + V_{0z} \frac{d}{dz} \right] n = -\omega_p^2 \left(i \frac{\omega}{c} + \frac{d}{dz} \right) v_z. \quad (14)$$

Assume now that the various natural frequencies characterizing the electron beam (such as ω_p and $\Omega = e\mathbf{B}_0/mc\gamma$) are much less than ω . Then we expect the spatial variation of \mathbf{a} , \mathbf{b} , \mathbf{v} , and n to be on a scale slow compared to the fast oscillatory part $e^{i\omega z/c}$ in Eqs. (8)–(11). Namely, in order of magnitude, for $x = a, da/dz, v, n$:

$$\left| \frac{d \ln x}{dz} \right| \ll \frac{\omega}{c}. \quad (15)$$

With this assumption we can rewrite Eqs. (12)–(14) in the following approximate form:

$$\frac{d\mathbf{a}_\perp}{dz} = \frac{1}{2c^3} (\omega_p^2 \mathbf{v}_\perp + \mathbf{V}_{0\perp} n), \quad (16)$$

$$a_z = i \frac{n}{\omega c}, \quad (17)$$

$$\frac{1}{c} \left[i\omega \left(\frac{V_{0z}}{c} - 1 \right) + V_{0z} \frac{d}{dz} \right] n = -i \frac{\omega_p^2 \omega}{c} v_z. \quad (18)$$

III. MOMENTUM EQUATION

Consider now the momentum equation

$$\left(\frac{\partial}{\partial t} + V_z \frac{\partial}{\partial z} \right) (\gamma \mathbf{V}) = -\frac{e}{m} \left(\frac{\mathbf{V}}{c} \times [\mathbf{B} + \mathbf{B}(z,t)] + \mathbf{E}(z,t) \right). \quad (19)$$

In the absence of the electromagnetic fields, this equation describes a gyrating electron beam with

$$\mathbf{V}_0 = -w [\hat{\mathbf{e}}_x \cos(k_0 z + \phi) + \hat{\mathbf{e}}_y \sin(k_0 z + \phi)] + u \hat{\mathbf{e}}_z, \quad (20)$$

where $u, w = \text{Const}$; $k_0 = e\mathbf{B}_0/mc\gamma u = \Omega/u$ and ϕ defining the velocity of the beam at $z = 0$. With no loss of generality let us assume that $\phi = 0$ and define a rotating coordinate system with the base vectors

$$\hat{\mathbf{e}}_1 = -\hat{\mathbf{e}}_x \sin k_0 z + \hat{\mathbf{e}}_y \cos k_0 z, \quad (21)$$

$$\hat{\mathbf{e}}_2 = -\hat{\mathbf{e}}_x \cos k_0 z - \hat{\mathbf{e}}_y \sin k_0 z, \quad (22)$$

$$\hat{\mathbf{e}}_3 = \hat{\mathbf{e}}_z. \quad (23)$$

Then $\mathbf{V}_0 = w\hat{\mathbf{e}}_2 + u\hat{\mathbf{e}}_3$ and the linearized momentum equation for perturbed velocities, in components along $\hat{\mathbf{e}}_i$ ($i = 1, 2, 3$), becomes

$$\begin{aligned} \frac{1}{c} \left[i\omega \left(\frac{u}{c} - 1 \right) + u \frac{d}{dz} \right] v_1 \\ = k_0 w \left(\frac{u\Gamma}{c^2 \gamma_0} + \frac{v_3}{c} \right) + \frac{1}{\gamma_0} \left(\frac{u}{c} b_2 - a_1 \right), \end{aligned} \quad (24)$$

$$\frac{1}{c} \left[i\omega \left(\frac{u}{c} - 1 \right) + u \frac{d}{dz} \right] v_2 = -w \frac{\Gamma'}{c^2 \gamma_0} - \frac{1}{\gamma_0} \left(\frac{u}{c} b_1 + a_2 \right), \quad (25)$$

$$\frac{1}{c} \left[i\omega \left(\frac{u}{c} - 1 \right) + u \frac{d}{dz} \right] v_3 = u \frac{\Gamma'}{c^2 \gamma_0} + \frac{1}{\gamma_0} \left(\frac{w}{c} b_1 - a_3 \right), \quad (26)$$

where similar to Eqs. (8)–(11) we defined

$$\gamma = \gamma_0 + \text{Re}(\Gamma(z) e^{i\omega(z/c - t)}), \quad (27)$$

and

$$\Gamma' = \frac{1}{c} \left[i\omega \left(\frac{u}{c} - 1 \right) + u \frac{d}{dz} \right] \Gamma. \quad (28)$$

The energy conservation equation

$$\frac{d\gamma}{dt} = -\frac{e}{mc^2} (V_1 E_1 + V_2 E_2 + V_3 E_3), \quad (29)$$

can be employed, to get on linearization

$$\Gamma' = -\frac{w}{c} a_2 - \frac{u}{c} a_3. \quad (30)$$

Finally, in the new coordinates, the field and density Eqs. (16)–(18) become

$$\frac{da_1}{dz} - k_0 a_2 = \frac{\omega_p^2 v_1}{2c^3}, \quad (31)$$

$$\frac{da_2}{dz} + k_0 a_1 = \frac{1}{2c^3} (\omega_p^2 v_2 + wn), \quad (32)$$

$$a_3 = i \frac{n}{\omega c}, \quad (33)$$

$$\frac{1}{c} \left[i\omega \left(\frac{u}{c} - 1 \right) + u \frac{d}{dz} \right] n = -i \frac{\omega_p^2}{c} v_3. \quad (34)$$

Equations (24)–(26), (30), and (31)–(34) comprise a system of first-order, linear, ordinary differential equations, describing our system completely for any given set of initial conditions at $z = 0$. Note that due to the choice of the base vectors $\hat{\mathbf{e}}_i$ ($i = 1, 2, 3$) we have a system of equations with constant coefficients, which allows us to seek the solution in

the form $\psi(z) = \psi_k \exp(ikz)$, where ψ stands for $v_i, a_i, b_i (i = 1, 2, 3)$, Γ and n . Then Eqs. (24)–(26) become

$$i\Delta v_{1k} = \frac{wk_0}{c} v_{3k} + \frac{wuk_0}{c^2\gamma_0} \Gamma_k + \frac{1}{\gamma_0} \left(\frac{u}{c} b_{2k} - a_{1k} \right), \quad (35)$$

$$i\Delta v_{2k} = -i\Delta \Gamma_k \frac{w}{c\gamma_0} - \frac{1}{\gamma_0} \left(\frac{u}{c} b_{1k} + a_{2k} \right), \quad (36)$$

$$i\Delta v_{3k} = -i\Delta \Gamma_k \frac{u}{c\gamma_0} + \frac{1}{\gamma_0} \left(\frac{w}{c} b_{1k} - a_{3k} \right), \quad (37)$$

where

$$\Delta = \frac{\omega}{c} \left(\frac{u}{c} - 1 \right) + k \frac{u}{c}. \quad (38)$$

Similarly Eq. (30) reduces to

$$i\Delta \Gamma_k = -\frac{w}{c} a_{2k} - \frac{u}{c} a_{3k}, \quad (39)$$

and the field and density Eqs. (31)–(34) give

$$ika_{1k} - k_0 a_{2k} = \frac{\omega_p^2}{2c^3} v_{1k}, \quad (40)$$

$$ika_{2k} + k_0 a_{1k} = \frac{1}{2c^3} (\omega_p^2 v_{2k} + wn_k), \quad (41)$$

$$a_{3k} = i \frac{n_k}{\omega c}, \quad (42)$$

$$\Delta n_k = -\frac{\omega_p^2 \omega}{c} v_{3k}. \quad (43)$$

Expressions for b_{1k} and b_{2k} in Eqs. (35)–(37) can be found from Eq. (4):

$$b_{1k} = -a_{2k} + \frac{ic}{\omega} (ika_{2k} + k_0 a_{1k}), \quad (44)$$

$$b_{2k} = a_{1k} - \frac{ic}{\omega} (ika_{1k} - k_0 a_{2k}). \quad (45)$$

On using Eqs. (40) and (41) on the left-hand sides of Eqs. (44) and (45), substituting the resulting expressions and Γ_k from Eq. (39) into the momentum Eqs. (35)–(37) and expressing a_{3k} through v_{3k} via Eqs. (42) and (43) we get

$$i \left(\Delta + \frac{\omega_p^2 u}{2\gamma_0 \omega c^2} \right) v_{1k} = \left(\frac{u}{c} - 1 \right) \frac{a_{1k}}{\gamma_0} + \frac{i\omega^2 u k_0}{\Delta c^3 \gamma_0} a_{2k} + \frac{wk_0}{c} \left[1 + \frac{\omega_p^2 u^2}{\Delta^2 c^4 \gamma_0} \right] v_{3k}, \quad (46)$$

$$i \left(\Delta + \frac{\omega_p^2 u}{2\gamma_0 \omega c^2} \right) v_{2k} = \left(\frac{w^2}{c^2} + \frac{u}{c} - 1 \right) \frac{a_{2k}}{\gamma_0} - \frac{i\omega_p^2 u w}{2\gamma_0 c^4 \Delta} v_{3k}, \quad (47)$$

$$(\Delta^2 - \xi^2) v_{3k} = i \frac{\Delta w (1 - u/c)}{c} \frac{a_{2k}}{\gamma_0} + \frac{\omega_p^2 w \Delta}{2\gamma_0 \omega c^2} v_{2k}, \quad (48)$$

where

$$\xi = \left[\frac{\omega_p^2}{c^2 \gamma_0} \left(1 - \frac{u^2}{c^2} - \frac{w^2}{c^2} \right) \right]^{1/2}, \quad (49)$$

is the plasma longitudinal response frequency. Assume now that

$$\frac{\omega_p^2 u}{2\gamma_0 \omega c^2 |\Delta|} \ll 1. \quad (50)$$

An *a posteriori* check of this assumption has shown that it is satisfied for all the numerical examples considered in this paper. Inequality (50) and additional assumptions of $w/c \leq 1/\gamma_0$ and $1 - u/c \ll 1$, which are consistent with our treatment of a high-frequency device, allow us to write the solutions of Eqs. (46)–(48) for $v_{ik} (i = 1, 2, 3)$ in the following approximate form:

$$v_{1k} = \frac{\omega^2 k_0 a_{2k}}{c^2 \Delta^2 \gamma_0} \left[1 + \frac{\omega_p^2}{\gamma_0 c^2} \frac{[1 - (u/c)][1 - (w^2/2c^2)]}{\Delta^2 - \xi^2} \right] + i \left(1 - \frac{u}{c} \right) \frac{a_{1k}}{\Delta \gamma_0}, \quad (51)$$

$$v_{2k} = \frac{ia_{2k}}{\Delta \gamma_0} \left[1 - \frac{u}{c} - \frac{w^2}{c^2} - \frac{\omega_p^2 u w^2 [1 - (u/c)]}{2c^4 \gamma_0 (\Delta^2 - \xi^2)} \right], \quad (52)$$

$$v_{3k} = \frac{i\Delta w [1 - (u/c)] a_{2k}}{c(\Delta^2 - \xi^2) \gamma_0}. \quad (53)$$

IV. STABILITY ANALYSIS AND NUMERICAL EXAMPLES

On substituting Eqs. (51)–(53) into the field equations (40) and (41), we can write the latter as

$$\epsilon_{11} a_{1k} + \epsilon_{12} a_{2k} = 0, \quad (54)$$

$$\epsilon_{21} a_{1k} + \epsilon_{22} a_{2k} = 0,$$

where the dielectric tensor is

$$\epsilon_{11} = ik - \frac{i\omega_p^2 (1 - u/c)}{2c^2 \gamma_0 \Delta}, \quad (55)$$

$$\epsilon_{12} = -k_0 - \frac{\omega_p^2 w^2 k_0}{2\gamma_0 c^4 \Delta^2} \left[1 + \frac{\omega_p^2 (1 - u/c)}{\gamma_0 c^2 (\Delta^2 - \xi^2)} \right], \quad (56)$$

$$\epsilon_{21} = k_0, \quad (57)$$

$$\epsilon_{22} = ik - \frac{i\omega_p^2}{2c^2 \gamma_0 \Delta} \left[1 - \frac{u}{c} - \frac{w^2}{c^2} - \frac{\omega w^2 \Delta (1 - u/c)}{c^3 (\Delta^2 - \xi^2)} \right]. \quad (58)$$

Existence of a nontrivial solution of Eq. (54) for a_{1k}, a_{2k} requires

$$D = \epsilon_{11} \epsilon_{22} - \epsilon_{12} \epsilon_{21} = 0, \quad (59)$$

which is the dispersion relation governing our system.

When the beam density goes to zero, the dielectric tensor becomes $\epsilon_{11} = \epsilon_{22} = ik$, $\epsilon_{21} = -\epsilon_{12} = k_0$. The dispersion relation in this case yields $k = \pm k_0$, which, of course, is the vacuum solution. This suggests, that for $\omega_p^2 \neq 0$, but small enough, we can treat the terms proportional to ω_p^2 in the expressions for ϵ_{ij} , as small perturbations and seek solutions for k in the form $k = \pm k_0 + x$, where $|x| \ll k_0$. We will use this perturbative approach in the rest of the paper.

First let $k = -k_0 + x$. Then if $\omega/c \simeq 2k_0 \gamma^2$, Δ is the order of k_0 and therefore $\Delta^2 - \xi^2 \simeq k_0^2$, so that the resonance denominators in Eqs. (56) and (58) are relatively large. The solution for x in this case is real, the mode is stable and does not contribute to the possible amplification in our system. Consider now the case $k = k_0 + x$. The values of Δ in this case will be of the order of x , if again $\omega/c \simeq 2k_0 \gamma^2$, and the resonance denominator $\Delta^2 - \xi^2$ in Eqs. (56) and (58) may

become very small. The dispersion relation now has the following approximate form:

$$(\beta - \Delta)(\Delta^2 - \xi^2) + \frac{1}{4}\xi^2\xi'^2\mu = 0, \quad (60)$$

where

$$\beta = \frac{\omega}{c} \left(\frac{u}{c} - 1 \right) + k_0 \frac{u}{c}, \quad (61)$$

$$\beta' = \beta + k_0 \left(1 - \frac{u}{c} \right), \quad (62)$$

$$\mu = \beta' - k_0 \frac{\xi'^2}{\Delta^2}, \quad (63)$$

and $\xi = w\gamma_0/c$.

The dispersion relation (60) has some features similar to the case of a conventional free electron laser. The similarity is expressed in the fact that as in the free electron lasers Eq. (60) describes the coupling between the electromagnetic ($\Delta \simeq \beta$) and beam ($\Delta \simeq \pm \xi$) modes and $\xi\xi'$ can be viewed as the parameter characterizing the strength of the coupling. Moreover, Eq. (60) reduces to the dispersion relation for the free electron laser³ if we set $\mu = -2k_0$. Note, that for $\Delta \ll \beta$ and ξ^2 small enough, Eq. (60) predicts a solution at $\Delta \simeq \xi$. Then $\mu \simeq -k_0$ and we can expect in this regime to have a solution of (60) for Δ similar to the solution we have in a free electron laser with the same values of k_0 , γ_0 , and the beam density twice lower than in our device. Together with these similarities, the apparent difference from the case of a free electron laser is in a more complicated form of μ which leads in our case to the higher-order dispersion relation and, as will be shown below, to coexistence of more than one unstable modes.

We now present some numerical examples. Figure 1 shows the calculated growth rates of the two unstable

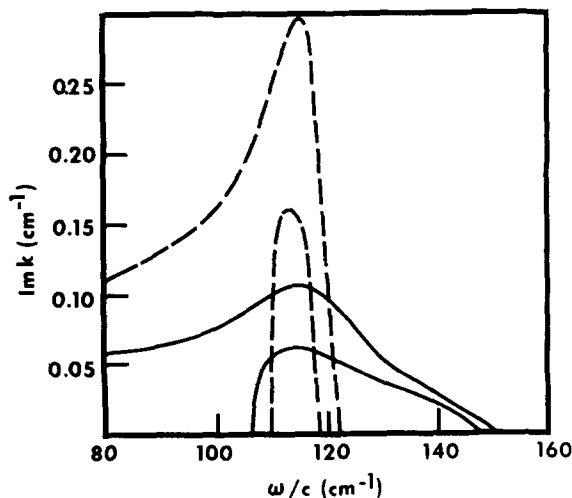


FIG. 1. Spatial growth rates Imk vs normalized frequency ω/c . The parameters are $\omega_p^2/c^2 = 2 \text{ cm}^{-2}$ and $k_0 = 3 \text{ cm}^{-1}$, $\gamma_0 = 5$ (solid lines) and $k_0 = 18.75 \text{ cm}^{-1}$, $\gamma_0 = 2$ (dashed lines). For each set of parameters, two unstable modes are present in the system.

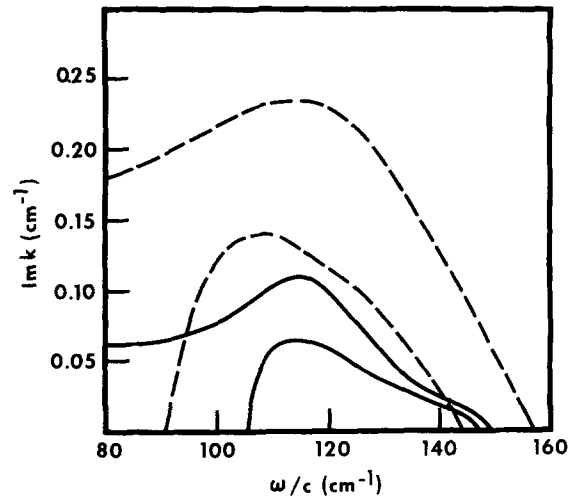


FIG. 2. Spatial growth rates Imk vs normalized frequency ω/c . The parameters are $\gamma_0 = 5$, $k_0 = 3 \text{ cm}^{-1}$, and $\omega_p^2/c^2 = 2 \text{ cm}^{-2}$ (solid lines) and $\omega_p^2/c^2 = 20 \text{ cm}^{-2}$ (dashed lines).

modes, which are present in the system, for fixed density of the beam and two different combinations of the strength of the axial magnetic field and the beam energy. The combinations were chosen so that $k_0\gamma^2$ in both cases remains the same. In addition we used $w/c = 0.1$ in both regimes. The comparison with the recent calculations for Raman free electron lasers,³ shows that for the case of higher energy of the beam ($\gamma_0 = 5$) the maximum growth rate in our system is about 30% lower than in the free electron laser with the same values of γ_0 , w , and ω_p^2 . If we use an approximate formula $Imk = w\omega_p/c^2(2\gamma_0)^{1/2}$ derived in Ref. 2 for the beam (1), we find that for $\gamma_0 = 5$ the gain in our system is ~40% higher. For the second set of parameters, with lower beam energy ($\gamma_0 = 2$), the maximum growth rate in our system becomes considerably higher than that predicted in Ref. 2 in this case ($Imk \simeq 0.1 \text{ cm}^{-1}$). In Fig. 2 we present the cases of two different beam densities, and fixed values of k_0 and γ_0 . Significant enhancement of the growth rate is evident with an increase of the beam density. For the higher density case ($\omega_p^2/c^2 = 20 \text{ cm}^{-2}$) the maximum growth rate is ~0.23 cm^{-1} as compared to ~0.13 cm^{-1} for the beam (1) in this case.

In summary, we have considered an amplifier based on the fully cold, guided, relativistic electron beam. It has been demonstrated that such a system may be superior to the device considered in Ref. 2. In the submillimeter regime the growth rates of the unstable modes in our system are comparable to those found in conventional free electron lasers. The use of only uniform guide magnetic fields allows one to explore electron beams with larger radial dimensions, as compared to those used in free electron lasers, where the best operation is obtained close to the axis of a magnetostatic scatterer. With all the aforementioned advantages, it is still necessary to find the best experimental methods of achieving the suggested configuration of the beam. The effects of a thermal spread in the beam on the growth rates in the sys-

tem, as well as nonlinear saturation effects also must be considered to provide better understanding of more realistic experimental situations.

ACKNOWLEDGMENTS

The authors would like to thank Professor I. B. Bernstein and Professor F. Dothan for their helpful comments and suggestions in the preparation of this paper. The authors also acknowledge the support in part by the U. S. Office of

Naval Research and by the U. S.-Israel Binational Science Foundation.

¹For a review of past work see P. Sprangle, R. A. Smith, and V. L. Granatstein, "Free Electron Lasers and Stimulated Scattering from Relativistic Electron Beams" in *Infrared and Millimeter Waves*, Vol. 1, edited by K. J. Button (Academic, New York, 1979), p. 279.

²J. L. Hirshfield, K. R. Chu, and S. Kainer, *Appl. Phys. Lett.* **33**, 847 (1978).

³L. Friedland and A. Fruchtman, *Phys. Rev. A* **25**, 2693 (1982).